Supplementary Information for

Highly enhanced upconversion luminescence in lanthanide-doped active-core/luminescent-shell/active-shell nanoarchitecture

Mingye Ding,[a] Daqin Chen, [a,]* Danyang Ma,[a] Jianbin Dai,[a] Yuting Li,[a] Zhenguo Ji[a]

[a] College of Materials and Engineering, Hangzhou Dianzi University, Hangzhou, 310018, P. R. China
* To Whom correspondence should be addressed.
E-mail: dqchen@hdu.edu.cn

1. Experimental section

Reagents: All of the chemical reagents used in this experiment are analytical grade and were received without further purification. $GdCl_3·6H_2O$ (99.99%), $YCl_3·6H_2O$ (99.99%), $YbCl_3·6H_2O$ (99.99%), $TmCl_3·6H_2O$ (99.995%), $ErCl_3·6H_2O$ (99.99%) and $HoCl_3·6H_2O$ (99.99%) were purchased from Beijing Founde Star Science & Technology Co., Ltd. NaOH (98%), NH_4F (98%), methanol (99.5%), and ethanol (99.7%) were provided by Sinopharm Chemical Reagent Co., Ltd. Oleic acid (OA, 90%), 1-octadecene (ODE, 90%) were received from Aladdin Reagent Company.

Synthesis of $NaGdF_4$:Yb core nanoparticles: In a typical experiment, $GdCl_3·6H_2O$ ($0.8 \times (1-x)$ mmol), $YbCl_3·6H_2O$ ($0.8 \times x$ mmol, x = 0, 0.2, 0.4, 0.6, 0.8, 1) were taken in a 50 mL three-necked flask at room temperature, and 8 mL of OA was added. The resulting mixture was then heated to 150 °C under a N_2 atmosphere and held at this temperature for 30 min to remove water from the homogeneous solution. Then, 12 mL ODE was quickly added to the flask and the resulted mixture was heated at 150 °C for another 30 min to form a clear solution. Subsequently, the flask was cooled down to 50 °C, and 10 mL methanol solution containing NH_4F (3 mmol), NaOH (2 mmol) was added dropwise and stirred at 50 °C for 30 min to ensure that all fluoride was consumed completely. The reaction temperature was then increased to 80 °C to remove the methanol from the reaction mixture. Upon removal of methanol, the solution was heated to 280 °C and maintained at this temperature under a nitrogen flow for 90 min, at which time the mixture was cooled down to room temperature. The resulting nanoparticles were precipitated out through an addition of ethanol, collected by centrifugation at 8000 rpm for 5 min, washed with ethanol and cyclohexane for several times, and finally re-dispersed in 6 mL cyclohexane.

Synthesis of $NaGdF_4$:Yb@$NaGdF_4$:Yb/Er core-shell nanoparticles: For synthesis of core/shell structure, $YbCl_3 \cdot 6H_2O$ (0.16 mmol), $ErCl_3 \cdot 6H_2O$ (0.016 mmol) and $YCl_3 \cdot 6H_2O$ (0.624 mmol) were added to a 50 mL three-necked flask containing 8 mL OA at room temperature. Then, the slurry was heated to 150 ^oC under a N_2 atmosphere with vigorous magnetic stirring for 30 min to form an optically transparent solution. A solution of ODE (12 mL) was then quickly added to the flask and the resulted mixture was heated at 150 ^oC for another 30 min. After the mixture was cooled down to 50 ^oC, the as-prepared core nanoparticles in 6 mL cyclohexane were added into the above solution and kept at 80 ^oC for 30 min. After the removal of cyclohexane, 10 mL methanol solution containing NH_4F (3 mmol) and NaOH (2 mmol). The resulting mixture was stirred at 50 ^oC for 30 min, at which time the reaction temperature was increased to 80 ^oC to remove the methanol. Then the solution was heated at 280 ^oC under a nitrogen flow for 90 min and finally cooled down to room temperature. The resulting core-shell nanoparticles were precipitated out by the addition of ethanol, collected by centrifugation, washed with ethanol and cyclohexane for several times, and finally and finally re-dispersed in 12 mL cyclohexane.

Synthesis of $NaGdF_4$:Yb@$NaGdF_4$:Yb/Er@$NaGdF_4$:Yb core-shell-shell nanoparticles: The core-shell-shell nanaoparticles were synthesized using a procedure similar to the one for core-shell nanoparticles. In a typical experiment, $GdCl_3 \cdot 6H_2O$ (0.8 × (1-y) mmol), $YbCl_3 \cdot 6H_2O$ (0.8 × y mmol, y = 0, 0.2, 0.4, 0.6, 0.8, 1) were added to a 50 mL three-necked flask containing 8 mL OA at room temperature. Then, the slurry was heated to 150 ^oC under a N_2 atmosphere with vigorous magnetic stirring for 30 min to form an optically transparent solution. A solution of ODE (12 mL) was then quickly added to the flask and the resulted mixture was heated at 150 ^oC for another 30 min. After the mixture was cooled down to 50 ^oC, the as-prepared core-shell nanoparticles in 6 mL cyclohexane were added into the above solution and kept at 80 ^oC for 30 min. After the removal of cyclohexane, 10 mL methanol solution containing NH_4F (3 mmol) and NaOH (2 mmol). The resulting mixture was stirred at 50 ^oC for 30 min, at which time the reaction temperature was increased to 80 ^oC to remove the methanol. Then the solution was heated at 280 ^oC under a nitrogen flow for 90 min and finally cooled down to room temperature. The resulting core-shell-shell nanoparticles were precipitated out by the addition of ethanol, collected by centrifugation, washed with ethanol and cyclohexane for several times, and finally and finally re-dispersed in 12 mL cyclohexane.

Characterization: Powder X-ray diffraction (XRD) measurements were performed on an AXS D8

advance diffractometer at a scanning rate of 10 °/min in the 2θ range from 10° to 80° with Cu Kα radiation (λ=0.15406 nm). Transmission electron microscopy (TEM) and selected area electron diffraction (SAED) patterns were recorded on JEM-200CX with a field emission gun operating at 200 kV. Images were acquired digitally on a Gatan multiple CCD camera. UC emission spectra were recorded with an Edinburgh Instruments FS5 fluorescence spectrophotometer equipped with an adjustable 980 nm laser diode module (MDL-III-980-1W, china) as excitation source. UC decay curves were measured with a customized UV to mid-infrared steady-state and phosphorescence lifetime spectrometer (FSP920-C, Edinburgh) equipped with a digital oscilloscope (TDS3052B, Tektronix) and a tunable mid-band OPO pulse laser as excitation source (410-2400 nm, 10 Hz, pulse width ≤ 5 ns, Vibrant 355II, OPOTEK). The effective decay time τ_{eff} is calculated by[1]

$$\tau_{eff} = \frac{1}{I_0}\int_0^{\infty} I(t)dt$$

where *I(t)* represents the luminescence intensity as a function of time *t* and I_0 denotes the maximum intensity. All the measurements were performed at room temperature.

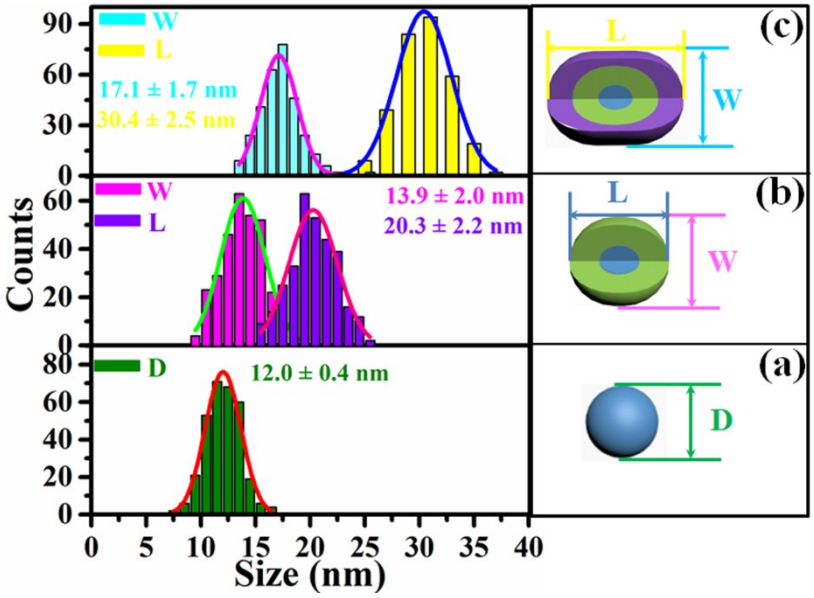

Figure S1. Histograms for the size distribution of (a) $NaGdF_4$:60%Yb^{3+} core , (b) $NaGdF_4$:60%Yb^{3+}@$NaYF_4$:20%Yb^{3+}/2%Er^{3+} core-shell and (c) $NaGdF_4$:60%Yb^{3+}@$NaYF_4$:20%Yb^{3+}/2%Er^{3+}@$NaGdF_4$:20%Yb^{3+} core-shell-shell nanoparticles.

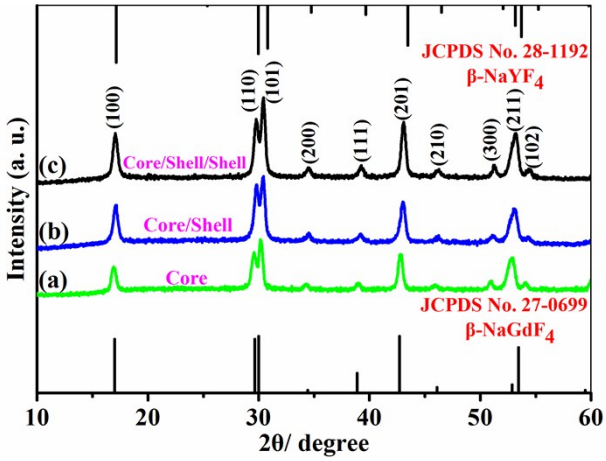

Figure S2. XRD patterns for (a) $NaGdF_4$:60%Yb^{3+} core, (b) $NaGdF_4$:60%Yb^{3+}@$NaYF_4$:20%Yb^{3+}/2%Er^{3+} core-shell and (c) $NaGdF_4$:60%Yb^{3+}@$NaYF_4$:20%Yb^{3+}/2%Er^{3+}@$NaGdF_4$:20%Yb^{3+} core-shell-shell nanoparticles. The standard data of hexagonal $NaGdF_4$ (JCPDS No. 27-0699) and hexagonal $NaYF_4$ (JCPDS No. 28-1192) is given as a reference.

The highly crystalline core, core-shell and core-shell-shell nanoparticles can be further confirmed by XRD analysis and selected electron diffraction (SAED) patterns. Figure S2 shows the XRD patterns of the as-synthesized $NaGdF_4$:Yb^{3+} core, $NaGdF_4$:Yb^{3+}@$NaYF_4$:Yb^{3+}/Er^{3+} core-shell and $NaGdF_4$:Yb^{3+}@$NaYF_4$:Yb^{3+}/Er^{3+}@$NaGdF_4$:Yb^{3+} core-shell-shell nanoparticles as well as the standard data of hexagonal $NaGdF_4$ (β-$NaGdF_4$) and hexagonal $NaYF_4$ (β-$NaYF_4$) for comparison. As shown, all the diffraction peaks for core, core-shell and core-shell-shell nanoparticles can be well indexed according to the standard data of the hexagonal $NaREF_4$ (RE = Y, Gd) phases (JCPDS No. 27-0699 and No. 28-1192), indicating the formation of pure β-$NaREF_4$ nanoparticles.[2] Figure S3 presents the SAED patterns of the as-obtained $NaGdF_4$:Yb^{3+} core, $NaGdF_4$:Yb^{3+}@$NaYF_4$:Yb^{3+}/Er^{3+} core-shell and $NaGdF_4$:Yb^{3+}@$NaYF_4$:Yb^{3+}/Er^{3+}@$NaGdF_4$:Yb^{3+} core-shell-shell nanoparticles. As shown in Figure S3, spotty polycrystalline diffraction rings, corresponding to the (100), (110), (200), (111), (201), (210) and (002) planes of hexagonal NaREF4 (RE = Gd, Y) lattice, can be clearly observed. The above results confirm the hexagonal-phase structure of all the three smaples.[3]

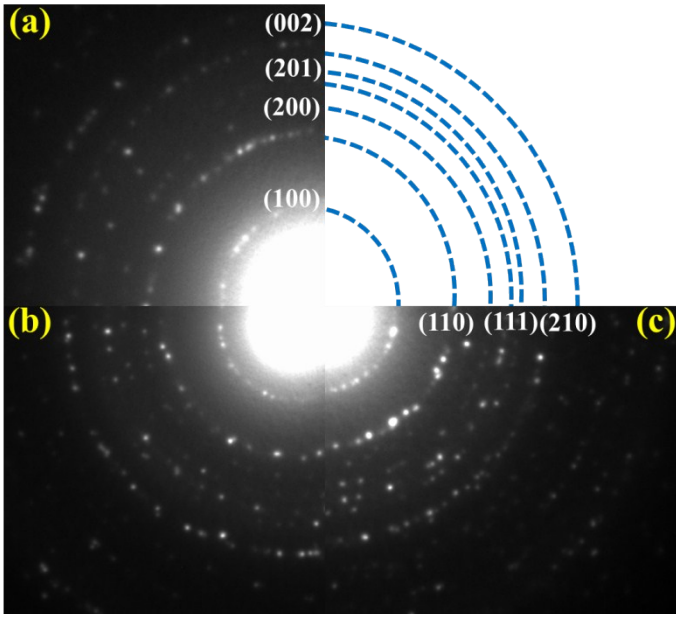

Figure S3. The selected area electron diffraction (SAED) spectra of (a) $NaGdF_4$:60%Yb^{3+} core, (b) $NaGdF_4$:60%Yb^{3+}@$NaYF_4$:20%Yb^{3+}/2%Er^{3+} core-shell and (c) $NaGdF_4$:60%Yb^{3+}@$NaYF_4$:20%Yb^{3+}/2%Er^{3+}@$NaGdF_4$:20%Yb^{3+} core-shell-shell nanoparticles.

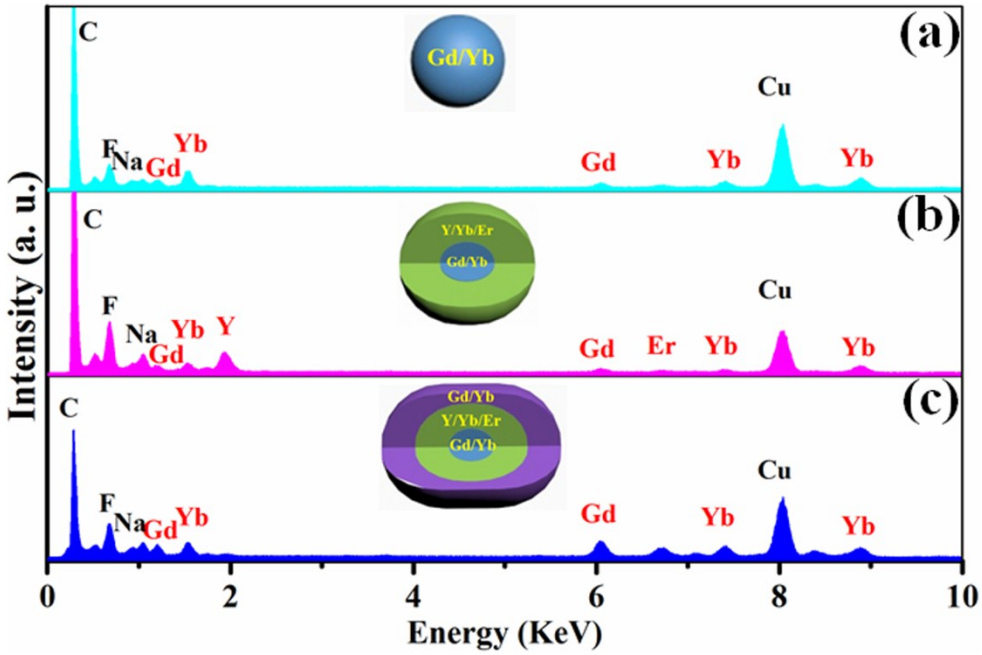

Figure S4. The energy-dispersive X-ray spectroscopy (EDS) analyses of (a) $NaGdF_4$:60%Yb^{3+} core, (b) $NaGdF_4$:60%Yb^{3+}@$NaYF_4$:20%Yb^{3+}/2%Er^{3+} core-shell and (c) $NaGdF_4$:60%Yb^{3+}@$NaYF_4$:20%Yb^{3+}/2%Er^{3+}@$NaGdF_4$:20%Yb^{3+} core-shell-shell nanoparticles.

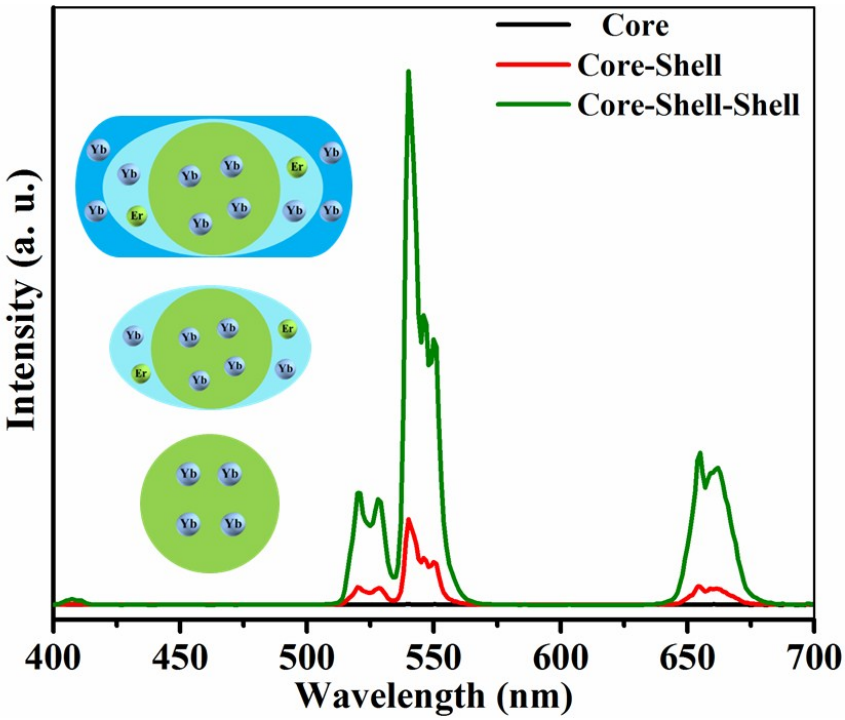

Figure S5. The upconversion emission spectra of the as-prepared $NaGdF_4$:60%Yb^{3+} core, $NaGdF_4$:60%Yb^{3+}@$NaYF_4$:20%Yb^{3+}/2%Er^{3+} core-shell and $NaGdF_4$:60%Yb^{3+}@$NaYF_4$:20%Yb^{3+}/2%Er^{3+}@$NaGdF_4$:20%Yb^{3+} core-shell-shell nanoparticles.

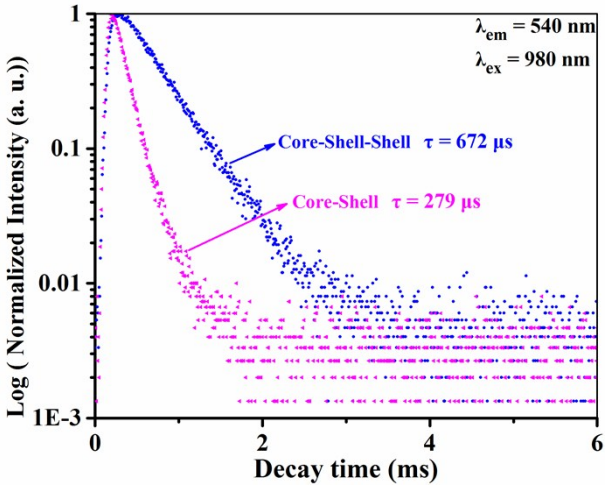

Figure S6. Decay curves of $^4S_{3/2} \rightarrow {}^4I_{15/2}$ transition of Er^{3+} ions for the corresponding $NaGdF_4$:60%Yb^{3+}@$NaYF_4$:20%Yb^{3+}/2%Er^{3+} core-shell and $NaGdF_4$:60%Yb^{3+}@$NaYF_4$:20%Yb^{3+}/2%Er^{3+}@$NaGdF_4$:20%Yb^{3+} core-shell-shell nanoparticles.

The UC emission spectra of the core, core-shell and core-shell-shell nanoparticles are shown in Figure S5. Under 980 nm laser excitation, no obvious emission peaks can be observed in the core sample. The $NaGdF_4$:40%Yb^{3+}@$NaYF_4$:20%Yb^{3+}, 2%Er^{3+} core-shell and $NaGdF_4$:40%Yb^{3+}@$NaYF_4$:20%Yb^{3+}, 2%Er^{3+}@$NaGdF_4$:20%Yb^{3+} core-shell-shell nanoparticles exhibit characteristic UC emission peaks, which can be assigned to $^2H_{11/2} \rightarrow {}^4I_{15/2}$ (521 nm), $^4S_{3/2} \rightarrow {}^4I_{15/2}$ (540 nm) and $^4F_{9/2} \rightarrow {}^4I_{15/2}$ (655 nm) transitions of Er^{3+}, respectively.[4] Evidently, the UC

emission intensity of core-shell-shell nanoparticles is about 7 times stronger than that of the core-shell sample. To further prove the UC enhancement more theoretically, the emission decay curves of $^4S_{3/2} \rightarrow {}^4I_{15/2}$ transition (540 nm) in core-shell and core-shell-shell nanoparticles are measured at the excitation of 980 nm, as shown in Figure S6. As shown, the lifetimes of $^4S_{3/2}$ state for core-shell and core-shell-shell samples are determined to be 279 μs and 672 μs, respectively. The results also provide strong evidence that the core-shell-shell nanoparticles have highly efficient UC luminescence.

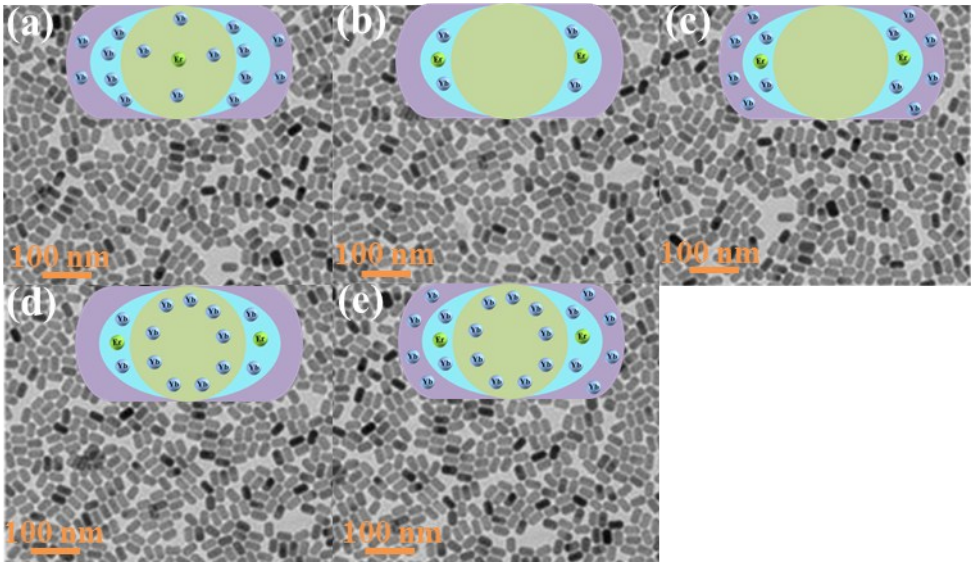

Figure S7. TEM images of Yb/Er@Yb@Yb, @Yb/Er@, @Yb/Er@Yb, Yb@Yb/Er@ and Yb@Yb/Er@Yb nanopartilces.

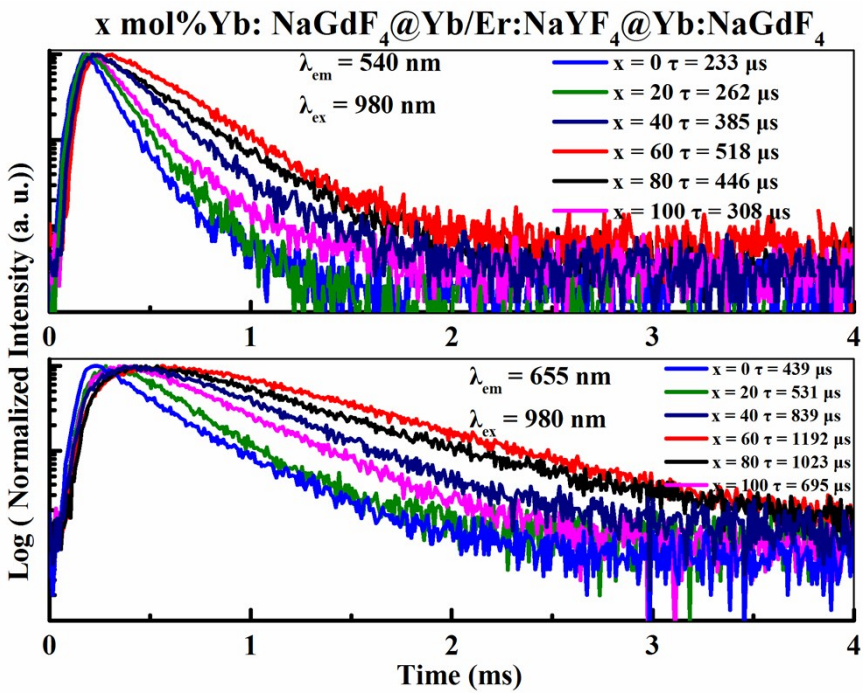

Figure S8. Decay curves of $^4S_{3/2} \rightarrow {}^4I_{15/2}$ and $^4F_{9/2} \rightarrow {}^4I_{15/2}$ transitions of Er^{3+} ions for the as-prepared $NaGdF_4$:x%Yb^{3+}@$NaYF_4$:20%Yb^{3+}/2%Er^{3+} @$NaGdF_4$:40%Yb^{3+} nanoparticles.

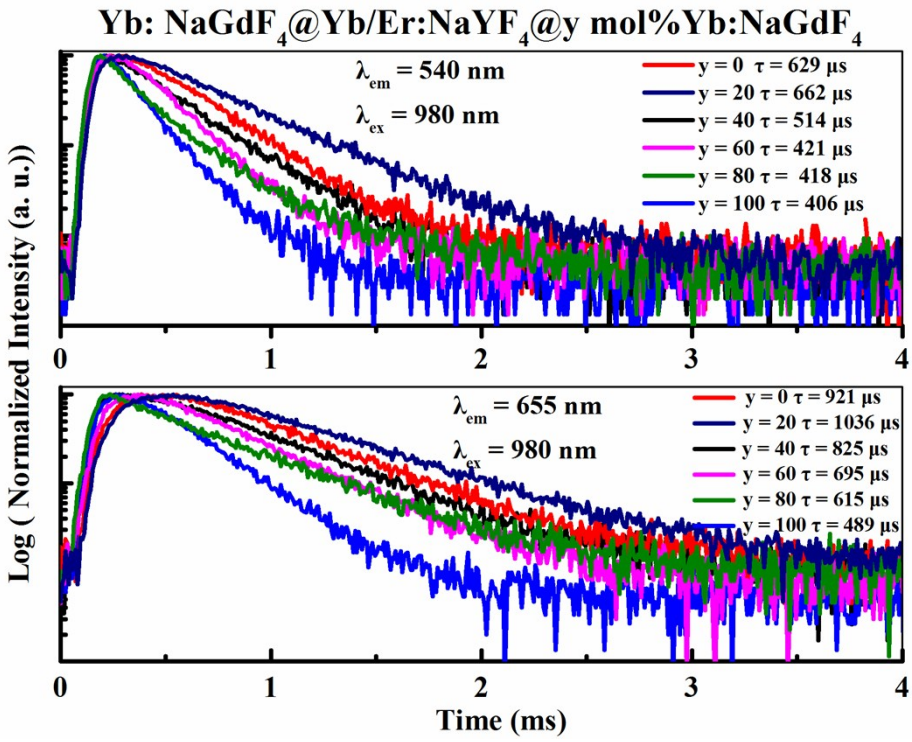

Figure S9. Decay curves of $^4S_{3/2} \rightarrow {}^4I_{15/2}$ and $^4F_{9/2} \rightarrow {}^4I_{15/2}$ transitions of Er^{3+} ions for the as-prepared $NaGdF_4$:60%Yb^{3+}@$NaYF_4$:20%Yb^{3+}/2%Er^{3+} @$NaGdF_4$:y%Yb^{3+} nanoparticles.

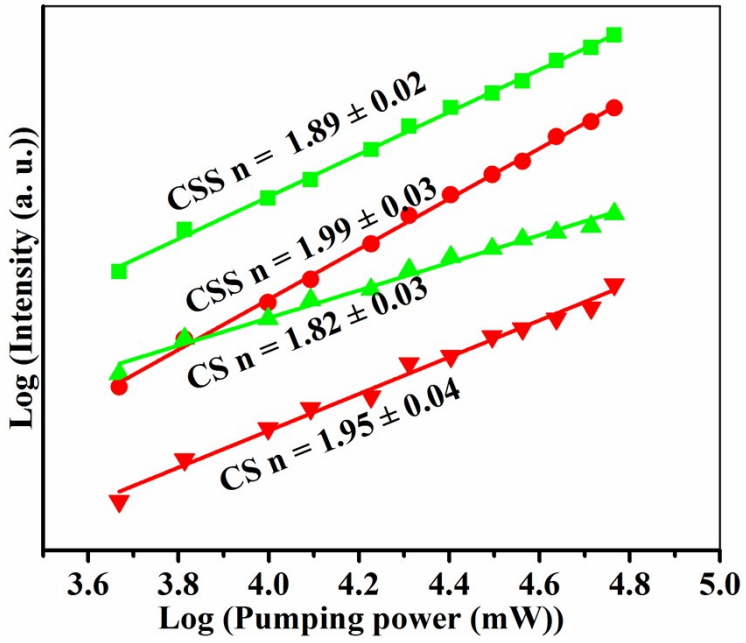

Figure S10. Pump power dependence of the UC emissions in $NaGdF_4$:40%Yb^{3+}@$NaYF_4$:20%Yb^{3+}/2%Er^{3+} core-shell (CS) and $NaGdF_4$:40%Yb^{3+}@$NaYF_4$:20%Yb^{3+}/2%Er^{3+}@$NaGdF_4$:20%Yb^{3+} core-shell-shell (CSS) nanoparticles.

The excitation power-dependent UC emissions of green ($^2H_{11/2}$, $^4S_{3/2} \rightarrow {}^4I_{15/2}$) and red ($^4F_{9/2} \rightarrow {}^4I_{15/2}$) for core-shell and core-shell-shell samples are calculated to deeply investigate the number of incident photons involved in the UC process. It is well known that the output UC luminescent intensity (I_{uc}) is proportional to the infrared excitation power (I_{IR}): (I_{IR}): $I_{uc} \propto (I_{IR})^n$, where n is the absorbed photon numbers per visible photon emitted, and its value can be obtained from the slope of the fitted line of the plot of log(I_{uc}) versus log(I_{IR}).[5] As shown in Figure S10, the slopes of the linear fits of $log(I_{uc})$ versus $log(I_{IR})$ for the green and red emissions in the core-shell-shell nanoparticles are 1.89 and 1.99, respectively, which is similar to that of the core-shell sample (1.82 and 1.95 for the green and red emissions), indicating that both green and red emissions are associated with two photon process.

References

1. Q. Su, S. Han, X. Xie, H. Zhu, H. Chen, C.-K. Chen, R.-S. Liu, X. Chen, F. Wang and X. Liu, *J. Am. Chem. Soc.*, 2012, 134, 20849-20857.

2. L. Lei, D. Chen, P. Huang, J. Xu, R. Zhang and Y. Wang, *Nanoscale*, 2013, 5, 11298-11305.

3. F. Chen, W. Bu, S. Zhang, X. Liu, J. Liu, H. Xing, Q. Xiao, L. Zhou, W. Peng, L. Wang and J. Shi, *Adv. Funct. Mater.*, 2011, 21, 4285-4294.

4. F. Auzel, *Chem. Rev.*, 2004, 104, 139-173.

5. N. Niu, P. Yang, F. He, X. Zhang, S. Gai, C. Li and J. Lin, *J. Mater. Chem.*, 2012, 22, 10889-10899.